

Analysis of Microstructure Impact on Electromigration

Hajdin Ceric, Roberto Lacerda de Orio, Johann Cervenka, and Siegfried Selberherr
Institute for Microelectronics, TU Wien, Gußhausstraße 27–29, A-1040 Wien, Austria
Email: {ceric|orio|selberherr}@iue.tuwien.ac.at

Abstract—The standard electromigration model is extended by introducing an anisotropic diffusivity which depends on the general stress tensor and a new model of grain boundaries which describes dynamics of mobile vacancies and vacancies trapped in grain boundaries. The application scenario for electromigration simulation is presented. The new calibration and usage concept takes into account microstructural diversity of interconnect inputs. A simulator example illustrating the effect of microstructural variation is presented and discussed.

I. INTRODUCTION

Introduction of advanced backend-of-line manufacturing process steps results in changed microstructures of the metal interconnects, types of interfaces structure, and new degradation phenomena. From accelerated electromigration tests carried out on dual-damascene copper structures it is known that for the same process parameters, geometry, and material choice the life time of the interconnect and the resistance change prior to failure are not unique but distributed over some range of values [1]. The source of this statistical character lays in the microstructure of copper and surface/interface defects. The microstructure of a metal is defined by the grain boundary network and crystal orientation inside the grains (texture). The state-of-the art experimental procedure for assessing properties of microstructures encompasses several techniques [2].

The grain size distribution can be precisely determined using AFM (Atomic Force Microscopy) and EBSD (Electron Backscatter Microscopy) [3], texture distribution with XRD (X-ray diffraction) and EBSD [2]. Furthermore, advanced experimental techniques enable a direct observation of the influence of layout geometry on the microstructure. It is a well established fact that a reduction in interconnect cross-section reduces the strength of (111) texture, which is preferred because of its good electromigration behavior. The choice of underlayer material [4] and overburden material [5] can significantly influence the texture quality.

Goal of this work is an impact analysis of the copper microstructure on primary electromigration effects, such as stress and vacancy distribution, which determine failure development. For this purpose a continuum model for electromigration induced material transport is extended by a model of grain boundaries in their double function, as fast diffusivity path and vacancy recombination site, respectively. Additionally, the interfaces to capping and barrier layer are also modeled as fast diffusivity paths [5].

II. EXTENDED ELECTROMIGRATION MODEL

Relaying on previous developments our model reveals an improvement in two major points, namely the complete integration of mechanical stress phenomena in the connection with microstructural aspects in the classical multi-driving force continuum model and the detailed treatment of grain boundary dynamics comprising both mobile and immobile vacancies.

Residual process stress, thermo-mechanical stress, and electromigration induced stress cause an anisotropy of material transport and, therefore, a tensorial diffusivity must be taken into account.

The framework for introduction of the model extensions is the bulk vacancy transport model which is given by the following balance equation

$$\frac{\partial C_v}{\partial t} = -\text{div} \mathbf{J}_v, \quad (1)$$

where \mathbf{J}_v is the vacancy flux driven by electromigration ($\sim \nabla \varphi$), the gradients of the vacancy concentration (∇C_v), and the mechanical stress ($\nabla \text{tr}(\bar{\sigma})$)

$$\mathbf{J}_v = -\mathbf{D}^v \left(\frac{Z^* e}{k_B T} C_v \nabla \varphi + \nabla C_v + \frac{f \Omega}{3 k_B T} C_v \nabla \text{tr}(\bar{\sigma}) \right). \quad (2)$$

Here, $k_B T$ is the thermal energy, $Z^* e$ is the effective valence, Ω is the volume of atom, and f is the vacancy to atom volume ratio. \mathbf{D}^v is the tensorial vacancy diffusivity which is in stress free state set as $D_{ij}^v = D_{bulk} \delta_{ij}$, where D_{bulk} is the isotropic bulk diffusivity.

III. THE EFFECT OF STRAIN

The choice of passivating film material and corresponding process technology causes tensile or compressive stress in the interface between the passivating film and the interconnect metal. Interfacial compressive stress diminishes electromigration along interfaces by reducing diffusivity [6]. However, numerous experimental observations have shown [7] that tensile stress in the interface increases the possibility of failure. Increased thickness and rigidity of the capping layer prevents relaxation of both thermal and electromigration induced stress, which results in dielectric cracking and metal extrusion. The local stress state introduces an anisotropy of the diffusivity. The dependence of the tensorial diffusivity on the stress state is given by the following relationship [8]:

$$D_{ij}^v = \frac{\Gamma_0}{2} \sum_{k=1}^{12} x_i^k x_j^k \exp\left(-\frac{\varepsilon_I^k \Omega (\mathbf{C}\varepsilon)}{k_B T}\right) \quad (3)$$

x_i^k is the i^{th} component of the jump vector \vec{r}^k for a site k , ε is the applied anisotropic strain, \mathbf{C} is the elasticity, ε_I^k is the strain induced by a single vacancy in the jump direction defined by the unit vector $\vec{n}_k = \vec{r}^k/|\vec{r}^k|$, and Γ_0 is the vacancy-atom exchange rate. The basis for this model, the relationship (3), was first presented in the theory of Dederichs *et al.* [9].

IV. THE GRAIN BOUNDARY MODEL

The basis for the actual understanding of vacancy dynamics in the presence of grain boundaries is Fisher's model [10]. This model includes two mechanisms: vacancy diffusion in the grain boundary and material exchange between the grain boundary and the grain bulk. During electromigration grain boundaries play an important role in stress relaxation. Therefore, Fisher's model is not sufficient for the complete description of grain boundary physics. The combination of Herring's [11] and Fisher's modeling approaches enables a certain insight in the vacancy dynamics in the presence of grain boundaries, however, for numerical implementation such a method is rather inconvenient.

We introduce a new model, where a grain boundary is treated as a separate medium with the capability of absorbing and releasing vacancies. Vacancies are trapped from both neighboring grains with the trapping rate ω_T and released to these grains with a release rate ω_R . The equilibrium vacancy concentration C_v^{eq} inside the grain boundary is determined by the local hydrostatic stress $p = -\text{tr}(\bar{\sigma})/3$

$$C_v^{eq} = C_v^0 \exp\left(-\frac{p\Omega}{k_B T}\right). \quad (4)$$

The vacancy production/annihilation term G is determined as the rate of change of immobile vacancies C_v^{im}

$$-G = \frac{\partial C_v^{im}}{\partial t} = \frac{1}{\tau} \left(C_v^{eq} - C_v^{im} \left(1 - \frac{2\omega_R}{\omega_T(C_{v,1} + C_{v,2})} \right) \right), \quad (5)$$

with

$$\frac{1}{\tau} = \frac{\omega_T(C_{v,1} + C_{v,2})}{\delta}. \quad (6)$$

In order to include the effect of the grain boundary as a vacancy sink (source) into the bulk vacancy transport model the recombination term G has to be included in equation (1). We obtain [12],

$$\frac{\partial C_v}{\partial t} = -\text{div}\mathbf{J}_v + G. \quad (7)$$

Equation (7) and the equation for the mechanical equilibrium [12] are solved inside the grain boundary. The flux \mathbf{J}_v is again calculated according to (2), but this time (stress free state) the diffusivity tensor is set as $D_{ij}^v = D_{gb}\delta_{ij}$. D_{gb} is the grain boundary diffusivity which is several orders of magnitude higher than D_{bulk} .

The full description of the atomic mechanisms of vacancy generation and annihilation in grain boundaries goes beyond the capability of continuum modeling and can only be obtained by molecular dynamics methods [13].

A. Numerical Realization of the Grain Boundary Model

Grain boundaries, and generally, every interface of the problem geometry have to be supplied with an appropriately fine mesh. This is necessary in order to provide sufficient resolution for the local dynamics described with the relationships (4)-(7).

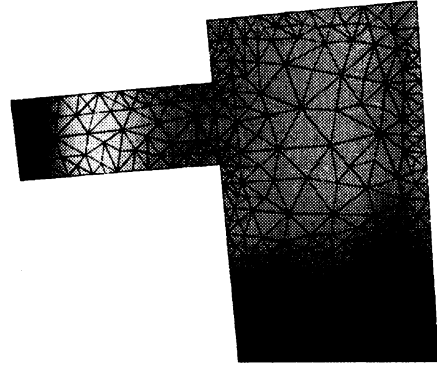


Fig. 1. The grain boundary plane is surrounded at both sides with slices spatially discretized with fine tetrahedra. In these slices high grain boundary diffusivities are set and at the same time the Rosenberg-Ohring term is activated.

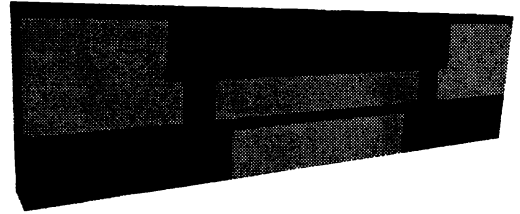


Fig. 2. Interconnect structure used for simulation.

V. USAGE SCENARIO FOR TCAD TOOLS

A satisfying assessment of electromigration reliability can only be achieved through a combination of experimental methods and the utilization of TCAD tools. Therefore, we discuss a possible usage scenario of TCAD tools in connection with results of accelerated interconnect tests. The proven scenario for application is:

- **Model Calibration.** For this purpose we use one layout and many test units. At the end of calibration all parameters of the model are fixed. During this process, different microstructures are used and simulation parameters are varied with the goal to reproduce experimental failure time statistics, Fig.3.

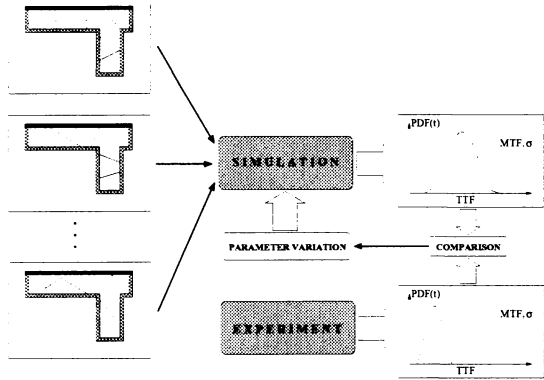


Fig. 3. Electromigration model calibration using a multitude of microstructural inputs.

- **Model Application.** The calibrated model is used for simulation. The simulation extrapolates the behavior of the interconnect under real life conditions.

For a given interconnect layout and monocrystalline material, simulation will provide a unique time-to-failure. All impact factors, e.g. geometry of the layout, bulk diffusivity, interface diffusivity, and mechanical properties are deterministic and so the time to failure is deterministic. However, the situation changes when the interconnect possesses a microstructure. The microstructure has a significant impact on electromigration, since it introduces a diversity of possible electromigration paths and local mechanical properties (the Young modulus and Poisson factor depend on the crystal orientation in each grain). However, the microstructure itself cannot be completely controlled by a process technology. In other words, the position of grain boundaries, angles in which they meet the interfaces, etc. cannot be designed, the process itself determines only statistics of grain sizes and textures.

VI. SIMULATION RESULTS AND DISCUSSION

We have applied our model to an interconnect layout which has been extensively used for accelerated electromigration tests for dual-damascene technologies. In order to properly include the effect of fast diffusivity paths, grain boundary, barrier, and capping layer diffusivities are set as $10^2 D_{bulk}$, $10^2 D_{bulk}$, and $10^5 D_{bulk}$, respectively.

The vacancy release rate ω_R and vacancy trapping rate ω_T are chosen in such a way that during simulation following conditions are fulfilled:

$$\frac{2\omega_R}{\omega_T(C_{v,1} + C_{v,2})} \ll 1, \quad (8)$$

and

$$1 \text{ s} < \tau = \frac{\delta}{\omega_T(C_{v,1} + C_{v,2})} < 2 \text{ s}. \quad (9)$$

With these conditions the model for immobile vacancies (4)-(6) behaves analogously to a classical Rosenberg-Ohring term [14], which was already successfully applied in [5].

The first of three microstructures (M1) used for simulation (Fig. 4) consists of grains of approximately equal size. The

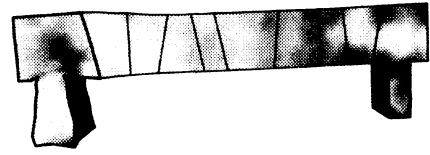


Fig. 4. Peak tensile stress distribution (dark areas) for the reference microstructure. The deformation of the interconnect on the left side is caused by a supersaturation of atoms (M1).

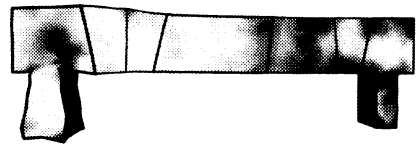


Fig. 5. Peak tensile stress for an unbalanced grain distribution (M2).

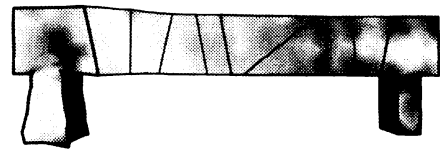


Fig. 6. Peak tensile stress for an unbalanced grain distribution (M3).

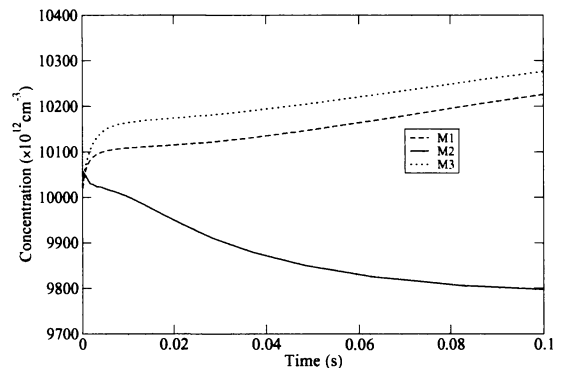


Fig. 7. Peak mobile vacancy concentration at triple points.

second one (M2) is obtained when the grain boundary in the middle is removed (Fig. 5). The stress and vacancy concentrations are monitored at the first triple point right from the removed grain boundary. The third structure (M3) (Fig. 6) is obtained by rotating the grain boundary around this triple point. The build up of tensile stress generally corresponds to

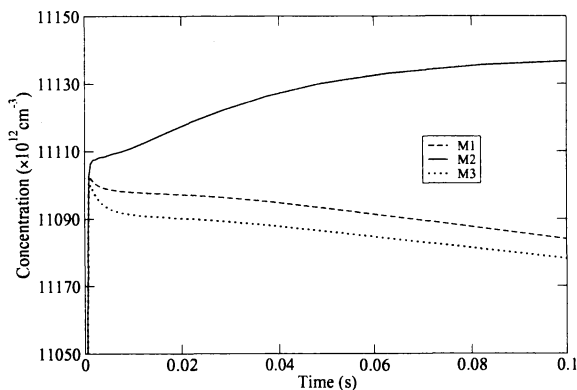


Fig. 8. Peak immobile vacancy concentration at triple points.

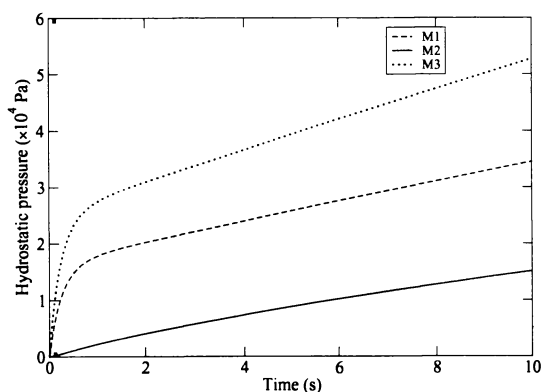


Fig. 9. Peak tensile stress dynamics for three different microstructures.

the dynamics of mobile and immobile vacancies. Initially, a strong increase of both types of vacancies is observed (Fig. 7 and 8). Later on, the stress in the structures M1 and M3 increases due to the increase of the mobile vacancies concentration, on the other hand, in structure M2, immobile vacancies are responsible for the stress increase. However, all three cases have a rather transitional character, after several seconds a quasi-steady state is reached where the stress linearly increases (Fig. 9) due to the linear increase of the immobile vacancy concentration. At the same time the concentration of mobile vacancies remains almost constant. The structure M3 exhibits not only the highest stress at the triple point but also has the highest gradient of stress increase. The reason for a such behavior is the larger surface of the grain boundary and a smaller angle between grain boundary and electron flow.

The coincidence of high vacancy concentration and high tensile stress regions with triple points indicates that triple points are natural locations of void nucleation. This assumption was also expressed in the discussion of results of accelerated electromigration tests published in [15].

The simulation results clearly indicate that an improvement of the failure behavior can be obtained by reducing the grain boundary surface and at the same time reducing its capability to absorb vacancies. The latter can be achieved by

a combination of impurity doping and interface strengthening [16].

VII. CONCLUSION

In order to obtain more accurate simulation results a standard electromigration model is extended by models for strain dependent anisotropic diffusivity and detailed model for grain boundaries. The concept of immobile and mobile vacancies enables a better understanding of stress build up and the role of triple points. The possible calibration and usage scenarios of electromigration tools are discussed. The physical soundness of the model is proved by three-dimensional simulations of typical dual-damascene structures used in accelerated electromigration testing.

ACKNOWLEDGMENT

Support by the Austrian Science Fund with the project P18825-N14 is gratefully acknowledged.

REFERENCES

- [1] A. von Glasow, "Zuverlässigkeitsaspekte von Kupfermetallisierungen in Integrierten Schaltungen," Dissertation, Technische Universität München, 2005.
- [2] M. A. Meyer, I. Zienert, and E. Zschech, "Electron Backscatter Diffraction: Application to Cu Interconnects in Top-View and Cross Section," *Materials for Information Technology*, vol. 1, no. 1, pp. 95–100, 2005.
- [3] E. Zschech and P. R. Besser, "Microstructure Characterization of Metal Interconnects and Barrier Layers: Status and Future," *Proc. of Interconnect Technol. Conf.*, pp. 233–235, 2000.
- [4] K. Abe, Y. Harada, and H. Onoda, "Study of Crystal Orientation in Cu Film on TiN Layered Structures," *J. Vac. Sci. Technol. B*, vol. 17, no. 4, pp. 1464–1469, 1999.
- [5] V. Sukharev, E. Zschech, and W. D. Nix, "A Model for Electromigration-Induced Degradation Mechanisms in Dual-Inlaid Copper Interconnects: Effect of Microstructure," *J. Appl. Phys.*, vol. 102, no. 5, pp. 530 501–530 514, 2007.
- [6] J. Lloyd and K. P. Rodbell, "Reliability," in *Handbook of Semiconductor Interconnection Technology*, edited by G.C. Schwartz and K. V. Srikishnan, pp. 471–520, 2006.
- [7] J. Lloyd and J.J. Clement, "Electromigration in Copper Conductors," *Thin Solid Films*, vol. 262, no. 1, pp. 135–141, 1995.
- [8] R. L. de Orío, H. Ceric, and S. Selberherr, "Effect of Strains on Electromigration Material Transport in Copper Interconnect Structures under Electromigration Stress," to be published in *J. Comp. Elect.*
- [9] P. H. Dederichs and K. Schroeder, "Anisotropic Diffusion in Stress Fields," *Phys. Rev. B*, vol. 17, no. 6, pp. 2524–2536, 1978.
- [10] J. C. Fisher, "Calculation of Diffusion Penetration Curves for Surface and Grain Boundary Diffusion," *J. Appl. Phys.*, vol. 22, no. 1, pp. 74–77, 1951.
- [11] C. Herring, "Surface Tension as a Motivation for Sintering," in *Physics of Powder Metallurgy*, edited by W. E. Kingston, pp. 143–179, 1951.
- [12] H. Ceric, R. Heinzl, C. Hollauer, T. Grasser, and S. Selberherr, "Microstructure and Stress Aspects of Electromigration Modeling," *Stress-Induced Phenomena in Metallization, AIP*, pp. 262–268, 2006.
- [13] M. R. Sorensen, Y. Mishin, and A. F. Voter, "Diffusion Mechanisms in Cu Grain Boundaries," *Phys. Rev. B*, vol. 62, no. 6, pp. 3658–3673, 2000.
- [14] R. Rosenberg and M. Ohring, "Void Formation and Growth During Electromigration in Thin Films," *J. Appl. Phys.*, vol. 42, no. 13, pp. 5671–5679, 1971.
- [15] E. Zschech and V. Sukharev, "Microstructure Effect on EM-Induced Copper Interconnect Degradation," *Microelectronic Engineering*, vol. 82, pp. 629–638, 2005.
- [16] M. Tada, M. Abe, N. Furutake, F. Ito, T. Tonegawa, M. Sekine, and Y. Hayashi, "Improving Reliability of Copper Dual-Damascene Interconnects by Impurity Doping and Interface Strengthening," *IEEE Elec. Dev.*, vol. 54, no. 8, pp. 1867–1877, 2007.